

ARTIFICIAL STRONTIUM AND BARIUM CLOUDS IN THE UPPER ATMOSPHERE

H. FÖPPL, G. HAERENDEL, L. HASER, J. LOIDL, P. LÜTJENS,
R. LÜST, F. MELZNER, B. MEYER, H. NEUSS and E. RIEGER
Max-Planck-Institut für Physik und Astrophysik, Institut für extraterrestrische Physik,
Garching bei München

(Received 24 September 1966)

Abstract—Experiments with strontium and barium vapour releases in the upper atmosphere, carried out in the Sahara and in Sardinia in 1964, are discussed.

(1) The yield of evaporated metal was tested for different chemical reactions. Sr proved to have efficiencies up to 40 per cent. For Ba a mixture of CuO and Ba gave the best results with a yield of nearly 7 per cent.

(2) No Sr ions were observed in the experiments. Barium, however, is strongly ionized. The ionization proceeds in two different steps: during the initial phase with a characteristic time of about 5 sec and by a slower photoionization process with a characteristic time of about 100 sec.

(3) The diameter of the neutral clouds increased as one would expect for purely molecular diffusion.

(4) The rate of increase in the central intensity of the clouds at sunrise was greater than the rate of decrease at sunset.

(5) Atmospheric wind velocities of $50\text{--}130\text{ msec}^{-1}$ were determined from the motion of the neutral clouds. The motion of the ion clouds perpendicular to the Earth's magnetic field indicated the presence of electric fields.

(6) The initial expansion velocity for explosive mixtures was greater by about a factor of four than the mean thermal velocity of the atoms at a temperature of about 3000°K .

1. INTRODUCTION

In an earlier paper (Föppl *et al.*, 1965) first results were given concerning the release of alkaline earth metal vapour in the upper atmosphere. Further experiments with sounding rockets have since been carried out and analysed.

The aims of these experiments are twofold: (1) to investigate the yield of different methods of evaporation (2) to study certain properties of the upper atmosphere. The observed neutral clouds give information about physical parameters of the neutral component of the atmosphere, whereas the behaviour of the ionized clouds depends in addition on the interaction with the ionized component of the atmosphere and on the magnetic and electric fields present here (Haerendel *et al.*, 1966). For studying those interactions and for deriving values for the strength and the direction of the electrical field it is necessary to measure the motions of the neutral and the ion clouds.

In this paper we mainly refer to the observational results of the expansion of the clouds in the initial and diffusional phase and to the motion of the neutral and ionized clouds as a whole. The theoretical background for the problem of the ambipolar diffusion of an ionized cloud in a magnetic field and the interpretation of the observed motion are given elsewhere (Haerendel *et al.*, 1966; Haerendel and Scholer, 1966).

2. CHARACTERISTICS OF THE ROCKET FLIGHTS

In the first paper results were given of seven experiments carried out in the Sahara in 1963 and in the Sahara and Sardinia 1964. This paper will refer to three series of experiments where 4 French Centaure, 1 French Dragon, and 2 British Skylark rockets were used.

French rockets were launched in the Algerian Sahara (Hammaguir) with the assistance of the Centre National d'Etudes Spatiales (CNES), and the Skylark rockets were launched by the European Space Research Organization (ESRO). The relevant data for the launchings are given in Table 1.

TABLE 1

No.	Date	Launch time	Launch site	Launch direction from north to east	Solar depression at take off	Range (km)	Height of evaporation (km)
1	14.2.64	5.57 UT	Sahara	15°	—13°	10	150
2	14.2.64	5.57 UT	Sahara	15°	—13°	10	170
3	15.2.64	5.57 UT	Sahara	325°	—13°	50	142
4	6.7.64	20.23 CET	Sardinia	95°	—6°	?	157
5	8.7.64	20.22 CET	Sardinia	95°	—6°	?	133
6	27.11.64	17.38 UT	Sahara	134°	—6.5°	70	152
7	30.11.64	17.37 UT	Sahara	132°	—6°	32	164
8	30.11.64	17.37 UT	Sahara	132°	—6°	32	200
9	3.12.64	17.40 UT	Sahara	110°	—7°	200	385

In the following we shall refer to the number of the experiment given in the first column.

3. METHODS OF EVAPORATION

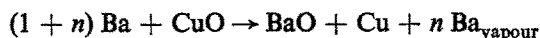
For these experiments two different chemical reactions were used in order to evaporate strontium (Sr) and barium (Ba). In all cases it was found that Ba is more difficult to evaporate than Sr. This is probably due to the lower vapour pressure of Ba as compared with Sr. In one reaction metal nitrate and magnesium (Mg) were used as reducing agent. These reactions had already been applied in the earlier experiments. Here the binder in which the chemicals are imbedded is of great importance. By this the burning time can be varied.

A silicon binder used in experiments 1, 4 and 5 gives a relatively slow burning time of the order of several seconds, depending on the total amount and the shape of the container.

A mixture of nitroglycerin and nitrocellulose called a POL-mixture was used as binder in experiment 6 and led to relatively long burning times of the order of 1–2 sec. This preparation has the disadvantage that only 30 per cent of the total weight consisted of the mixture of $\text{Ba}(\text{NO}_3)_2 + 6 \text{ Mg}$.

Higher efficiencies for the evaporation of Sr and Ba could be obtained with a binder of nitro-cellulose only. In this way very short burning times (smaller than 0.02 sec) were observed. Such a binder was used for the experiments 2, 3, 8 and 9.

Another completely different reaction used in the experiment 7, turned out to be the most efficient. Here barium was mixed together with copper oxide (CuO). According to the equation



the barium is partially burned and provides the heat for the evaporation of the rest of the Ba. The reaction $\text{Ba} + \text{CuO} \rightarrow \text{BaO} + \text{Cu}$ has a heat production of approximately 94 kcal/mole. About 60 kcal/mole are necessary for heating the components up to 2000°C. The remaining heat is sufficient to evaporate $\frac{2}{3}$ mole of Ba ($n = \frac{2}{3}$) and to bring the vapour to 2000°C. Accordingly the theoretical yield is 30 per cent. In reality the yield is considerably less, probably because of condensation in the nozzle and during the expansion.

The components of the mixture, namely splinters of Ba and finely powdered CuO, are mixed and pressed into the container under high pressure and without a binder. The reaction time is very short, in any case shorter than the time of outflow which is about 0.1 sec. Because of this short time, the heating of the container and therefore the loss of heat is small, and consequently there are no problems regarding the strength of the container. Besides this the pressure in the container during the reaction is only about 50 atm.

The data concerning the chemical mixtures used in the different experiments are summarized in Table 2.

TABLE 2

No.	Height (km)	Mixture	Binder	% of total weight	Weight of Mixt. (kg)	Moles metal vapour-izable	Burning time (sec)
1	150	$\text{Sr}(\text{NO}_3)_2 + 6 \text{ Mg}$	Silicone	22	3.12	5.9 Sr	≈ 90
2	170	$\text{Sr}(\text{NO}_3)_2 + 6 \text{ Mg}$	Collod.	5	1.05	2.8 Sr	< 0.02
3	142	$\text{Sr}(\text{NO}_3)_2 + 6 \text{ Mg}$	Collod.	5	1.00	2.7 Sr	< 0.02
4	157	$\text{Sr}(\text{NO}_3)_2 + \text{Ba}(\text{NO}_3)_2 + 12 \text{ Mg}$	Silicone	21.5	13.67	14.0 Sr 14.0 Ba	≈ 2
5	133	$\text{Ba}(\text{NO}_3)_2 + 6 \text{ Mg}$	Silicone	19.7	13.56	28.0 Ba	≈ 30
6	152	$\text{Ba}(\text{NO}_3)_2 + 6 \text{ Mg}$	POL	70	3.3	2.6 Ba	≈ 2
7	164	$\text{CuO} + 4/3 \text{ Ba}$	—	—	0.5	0.6 Ba	< 0.1
8	200	$\text{Ba}(\text{NO}_3)_2 + 6 \text{ Mg}$	Collod.	5	6.1	14.3 Ba	< 0.02
9	385	$\text{Sr}(\text{NO}_3)_2 + 6 \text{ Mg}$	Collod.	5	43.1	114.7 Sr	< 0.02

4. THE IONIZATION

In the experiments 6, 7 and 8 ionized barium was observed. The Ba^+ ions are generated in two different ways: during the initial phase with a characteristic time of about 5 sec, and by a slower photoionization process with a characteristic time of about 100 sec (Lütjens, 1966). The initial ionization is particularly effective since it gives rise to well-concentrated clouds with a width of a few km in the direction perpendicular to B. The cloud then expands only along the lines of force, until certain deformations become important (Haerendel *et al.*, 1966).

The mechanism leading to this initial ionization is not yet clear. The width of the ion clouds corresponds well to the product of the initial velocity of expansion times of a few seconds. It could be that the initial ionization starts from a metastable atomic level.

Probably this metastable level is a $6s5d^1D$ state which lies 1.4 eV above the groundstate. Solar radiation with a wavelength of 3260 Å is needed to ionize a Ba-atom from this metastable state. The flux density at 3260 Å is about a factor of 30 greater than the flux density at 2380 Å, which is the ionization limit of Ba from the groundstate.

Also the subsequent slow photoionization is much faster than has been estimated previously (Föppl *et al.*, 1965). The absorption starting from the ground level of Ba is strengthened by several auto-ionization lines below 2380 Å. But the oscillator strengths are far too weak to explain the observed characteristic time (Hudson, 1965). Also here the process might involve an intermediate level. Further details about the process of ionization will be given in a later paper (Haser, 1966).

5. OBSERVATIONAL EQUIPMENT

The clouds were observed from two different stations, a main observational station and a second one for triangulation. The distances between the two stations were 23.85 km, 114

km, and 176 km respectively for the three different launch series. The main station was equipped with a number of cameras for 35-mm film, with K24 cameras, with two spectrographs, and during the third series also with a television camera. The second observation station was equipped with K24 cameras only.

The cameras with 35-mm film had focal lengths of 40 mm and 50 mm and apertures of 1:1.9 and 1:2 respectively. They were operated with different interference filters for a number of spectral lines. One of the two-prism-spectrographs worked with a multiplier, the other one with a photographic plate. The television camera operated with an image orthicon in a preliminary set-up in order to compare its sensitivity with those of the photographic techniques.

6. THE YIELD OF THE EVAPORATION

As mentioned above, one aim of the experiments was to determine the yield of the different methods of evaporation. For this reason a determination of the total number of metal atoms contained in a cloud was attempted. This is possible if the cloud is optically thin, since in this case its intensity is proportional to the number of atoms along the lines of sight.

To determine the intensity the absolute sensitivity of the film must be known. This was measured by exposing the films to a light of constant intensity through a step reducer. The intensity of the light was measured before and after each exposure by a thermocouple whose sensitivity is known by measurements on a photometric standard (tungsten-ribbon lamp).

In a number of experiments the clouds which were initially optically thick became optically thin. Under these circumstances an independent estimate for the evaporated mass can be obtained from the expression for the optical thickness q .

$$q = N_{\perp} \frac{e^2}{m_e c} \cdot \sqrt{\left(\frac{m}{2kT}\right)} \cdot f_{mn} \cdot \lambda \quad (1)$$

where N_{\perp} = number of atoms per cm^2 along the line of sight

f_{mn} = oscillator strength of the transition

λ = wavelength of the transition.

This transition in optical thickness is indicated by a change in the shape of the cloud from a half moon to a sphere. At this instant q is not far from unity and one obtains

$$N_{\perp} = \frac{m_e c}{e^2} \sqrt{\left(\frac{2kT}{m}\right)} \frac{1}{f_{mn} \lambda} \quad (2)$$

If the cloud is spherical in a plane perpendicular to the line of sight and if the density distribution corresponds to a Gaussian curve, the total mass of the evaporated metal is given by

$$M_{\text{total}} = N_{\perp} \pi r_e^2 \quad (3)$$

Here r_e is the radius of the cloud where the intensity of the cloud is a factor e smaller than the maximum intensity.

A determination of the evaporated mass in this way has the advantage that no absolute calibration of the intensity is necessary and that it is not necessary to know the intensity of the solar radiation at the wavelength of the transition. In Table 3 the results obtained independently by the two methods are summarized.

The values of the evaporated masses determined by the two methods are in good agreement except for experiment 6. The Sr cloud of experiment 3 was always optically thick, as is shown in Fig. 1c. The 33 per cent efficiency stated in Table 3 was obtained by assuming

TABLE 3

No.	Element	Height (km)	Total mass (g) and yield (%)				Remarks
			Absolute method		Transition method		
			(g)	(%)	(g)	(%)	
3	Sr	142	—	—	200	33	—
4	Sr	155	—	—	11	0.9	—
4	Ba	155	—	—	—	—	—
6	Ba	150	1.1	0.8	3.3	2	Weather conditions not excellent
6	Ba ⁺	150	1.8		3.2		
6	Sr	150	0.36	20	1.2	67	Weather conditions not excellent
7	Ba	160	1.3	6.6	1.1	6.1	—
7	Ba ⁺	160	4.1		3.9		—
7	Sr	160	0.6	28	1	47	—
8	Ba	195	13.7	1	14	0.7	—
8	Ba ⁺	195	5.3		—		—
8	Sr	195	1.0	40	—	—	—
9	Sr	385	640	6.4	—	—	—

$q = 5$ and is quite uncertain. The experiments 6, 7, 8, and 9 gave a rather high efficiency of evaporated Sr compared with the evaporated Ba. This is probably due to the higher vapour pressure of Sr. It should be mentioned that Ba always contains some impurity of Sr (of the order of 0.1 per cent) which is always observed together with a barium cloud. The mass of evaporated Sr in experiment 4 is remarkably low, and Ba was not even noticeable. The reason for this is probably that the container broke up too early (the evidence for this assumption is the observed burning time of only 2 sec whereas the mixture should have burned for about 20 sec according to laboratory experiments).

From Table 3 it can be seen that the highest yield of evaporated barium is obtained with mixtures of barium and copper oxide. Later experiments to be described in another paper have confirmed the relatively high yield of this reaction. Experiments to determine the best proportions are in progress. Furthermore the influence of the shape of the nozzle, namely a laval nozzle and a ring nozzle, on the yield of free atoms is being studied.

7. THE INITIAL EXPANSION OF A CLOUD

After the evaporation the cloud expands rapidly until equilibrium with the surrounding atmosphere is reached and the diffusion of the cloud becomes important. The radius of the cloud at this instant is called the initial radius, r_i . It is either determined by the pressure balance between the cloud and the surrounding atmosphere or by the mean free path of the atmosphere. The latter becomes dominant at altitudes higher than about 140 km.

In Table 4 this initial radius r_i of some of the clouds is listed (r_i = radius when $J = \frac{1}{e} J_{\max}$).

TABLE 4

No.	Element	Height (km)	Initial radius r_i (km)
3	Sr	142	1.0 ± 0.3
4	Sr	157	2.8 ± 0.2
6	Sr	152	1.5 ± 0.2
6	Ba	152	2.4 ± 0.2

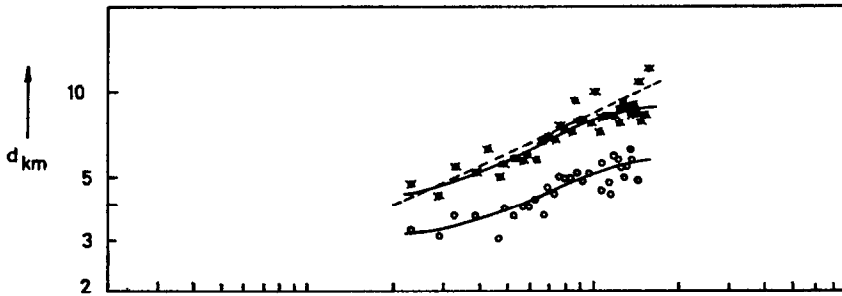


FIG. 1. (a). DIAMETER d OF THE CLOUD OF FEBRUARY 15, 1964, IN Sr I LIGHT AS A FUNCTION OF TIME.

$\circ \circ \circ$ $d^{0.75}$; $d^{0.75}$ = DIAMETER WHERE $J = 0.75 J_{\max}$
 $\times \times \times$ $d^{0.5}$; $d^{0.5}$ = DIAMETER WHERE $J = 0.5 J_{\max}$
 ——— LEAST SQUARE FIT TO THE DATA
 - - - THEORETICAL CURVE.

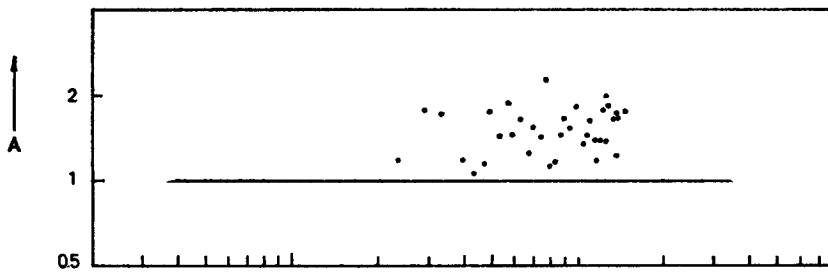


FIG. 1. (b). ASYMMETRY FACTOR $A = \frac{(r^{0.5} - r^{0.75})_{\text{away from Sun}}}{(r^{0.5} - r^{0.75})_{\text{to Sun}}}$

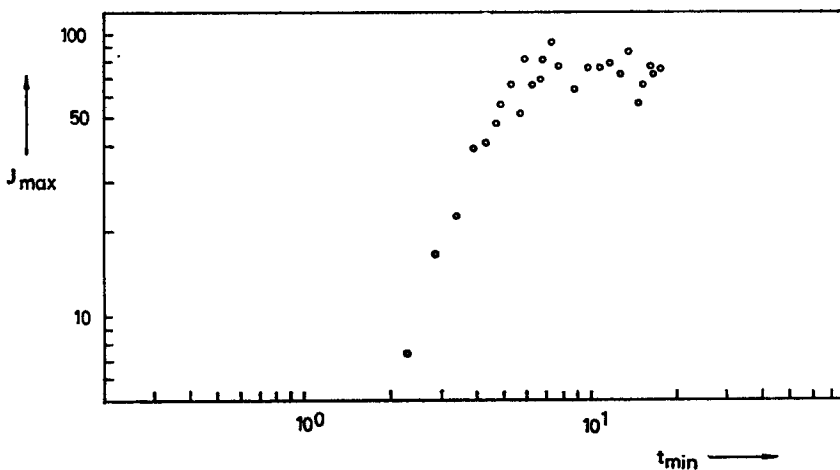


FIG. 1. (c). MAXIMUM INTENSITY OF THE CLOUD IN Sr I LIGHT AS A FUNCTION OF TIME.

In experiment 6 the radius of the Ba cloud was greater than the radius of the Sr cloud at the same altitude. This was also observed in a number of later experiments and is due to the higher mass of the barium atom as compared with strontium.

Only for experiment 9 which was carried out at a much higher altitude than the other experiments, was the initial phase of the expansion recorded. This will be discussed in section 10.

8. THE DIFFUSION OF A CLOUD

(a) *The time dependence*

After the initial expansion the cloud increases in size by diffusion into the surrounding atmosphere. For this phase diameters in the horizontal direction are plotted versus time for the phase of the diffusion in Figs. 1a, 2a, 3a and 4a. For purely molecular diffusion one would finally expect a time dependence of $t^{0.5}$. But the time dependence of the diameters deviates from this even long after the initial phase. The reason for this is the vertical

TABLE 5

No.	Element	Height (km)	Vertic. vel. (msec ⁻¹)	Initial rad. r_i (km)	D_0 (cm ² sec ⁻¹)	H_0
3	Sr	142	—	1.0 ± 0.3	(1 ± 0.3)10 ⁸	—
4	Sr	157	-13	2.8 ± 0.2	(2.5 ± 0.3)10 ⁸	20 ± 5
6	Sr	152	+15	1.5 ± 0.2	(2.5 ± 0.3)10 ⁸	20 ± 5
6	Ba	152	+15	2.4 ± 0.2	(2.5 ± 0.3)10 ⁸	20 ± 5

motion of the cloud as a whole. If the cloud moves upwards its diameter grows faster and if it moves downwards (which is more often the case) its diameter grows more slowly than with diffusion on the same height level. Of course the wind shear will also influence the development of the cloud, but this effect has not been considered here.

The time dependence of the diameter is tentatively expressed by the solution of the diffusion equation with a time-varying diffusion coefficient.

$$d = 2\sqrt{(\ln k)} \sqrt{\left(r_i^2 + 4 \int_0^t D(t') dt'\right)} \quad (4)$$

The influence of the pressure gradient has been neglected. Here $D(t)$ is the time-dependent diffusion coefficient and k a constant which is given by

$$K = 2 \text{ for } d^{0.5} (J = 0.5 J_{\max})$$

$$K = 1.33 \text{ for } d^{0.75} (J = 0.75 J_{\max})$$

In a one component isothermal atmosphere the diffusion coefficient varies with height as $D = D_0 e^{z/H_0}$. We express z by the observed vertical velocity: $\pm vt$ and obtain from (4):

$$d = 2\sqrt{(\ln k)} \sqrt{\left(r_i^2 \pm \frac{4D_0 H_0}{v} \left[\exp\left(\pm \frac{vt}{H_0}\right) - 1\right]\right)} \quad (5)$$

The upper sign is for the upward motion of the cloud and the lower sign for the downward motion. The parameters r_i , D_0 and H_0 are determined by fitting the equations to the measurements. They are listed in Table 5.

The cloud of experiment 3 was initially in the Earth's shadow and reached its full visibility

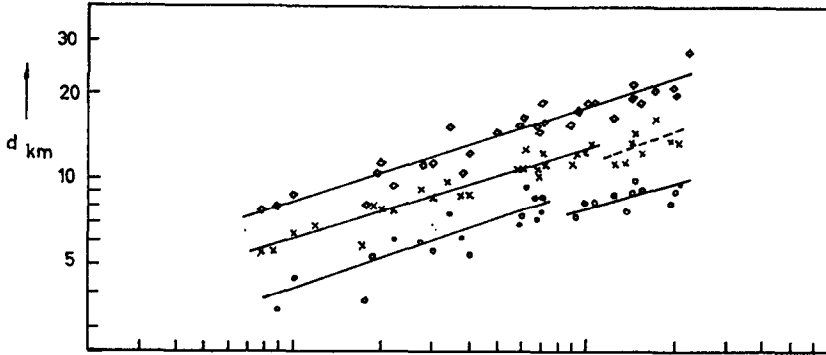


FIG. 2. (a). DIAMETER d OF THE CLOUD OF JULY 6, 1964, IN Sr I LIGHT AS A FUNCTION OF TIME.

○ ○ ○ $d^{0.75}$
 × × × $d^{0.5}$
 ◇ ◇ ◇ $d^{0.25}$

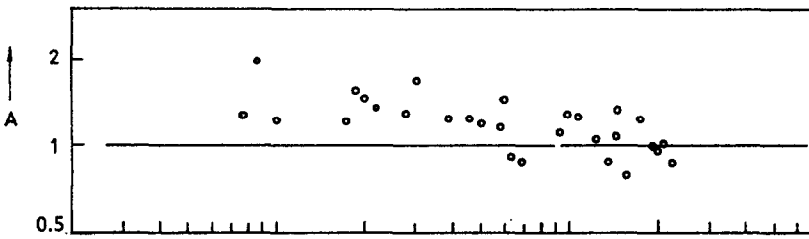


FIG. 2. (b). ASYMMETRY FACTOR A AS A FUNCTION OF TIME.

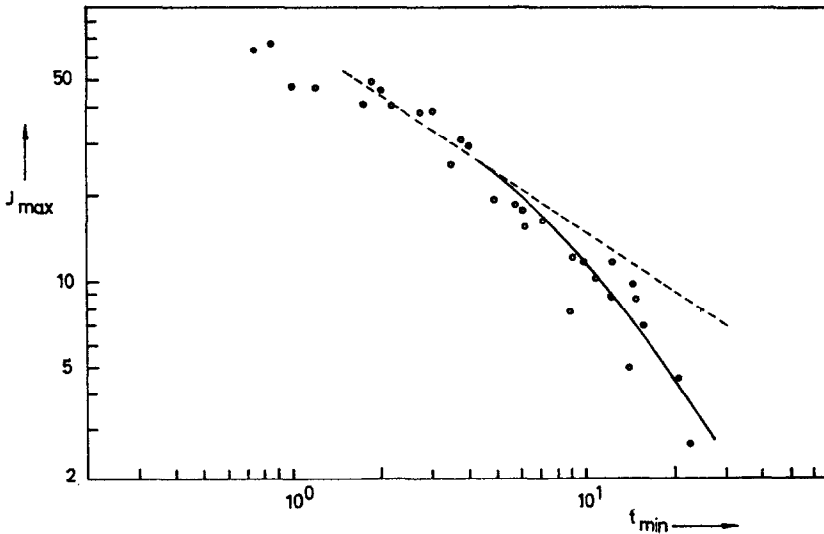


FIG. 2. (c). MAXIMUM INTENSITY OF THE CLOUD IN Sr I LIGHT AS A FUNCTION OF TIME.

— — — GEOMETRICAL DILUTION, $J_{\max} \sim t^{-0.68}$
 — — — LEAST SQUARE FIT TO THE DATA.

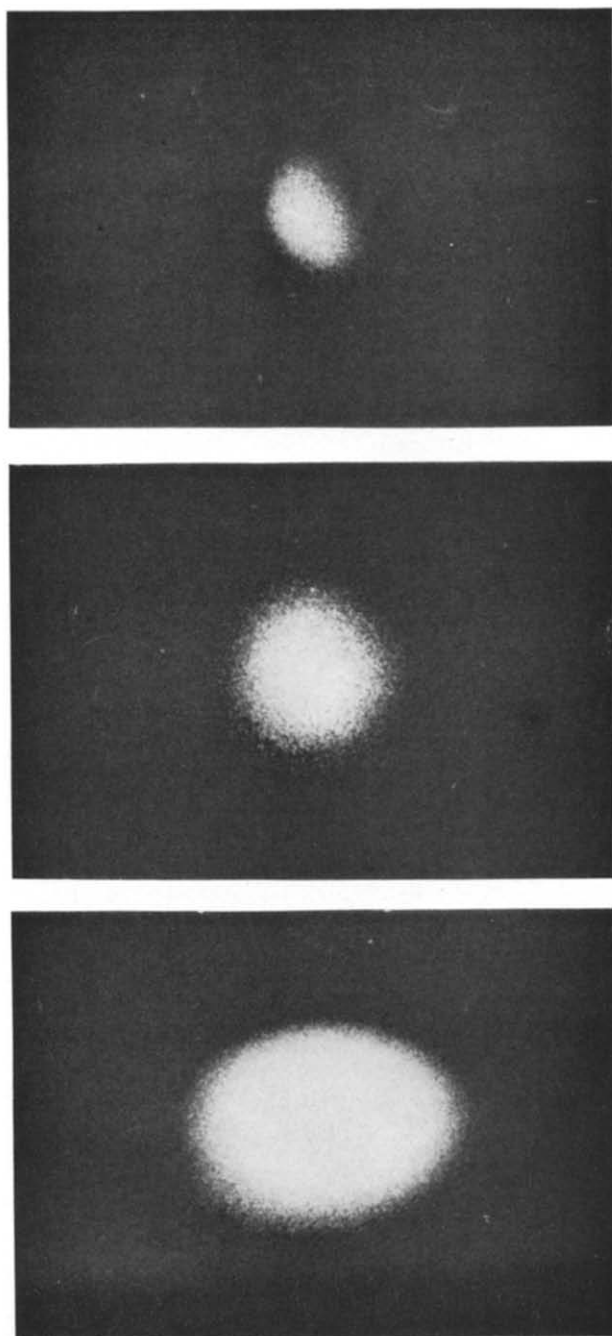


FIG. 2. (d). THE CLOUD OF JULY 6, 1964, IN Sr I LIGHT AS SEEN FROM LA MADDALENA 52 sec, 4 min, AND 22 min AFTER EVAPORATION.

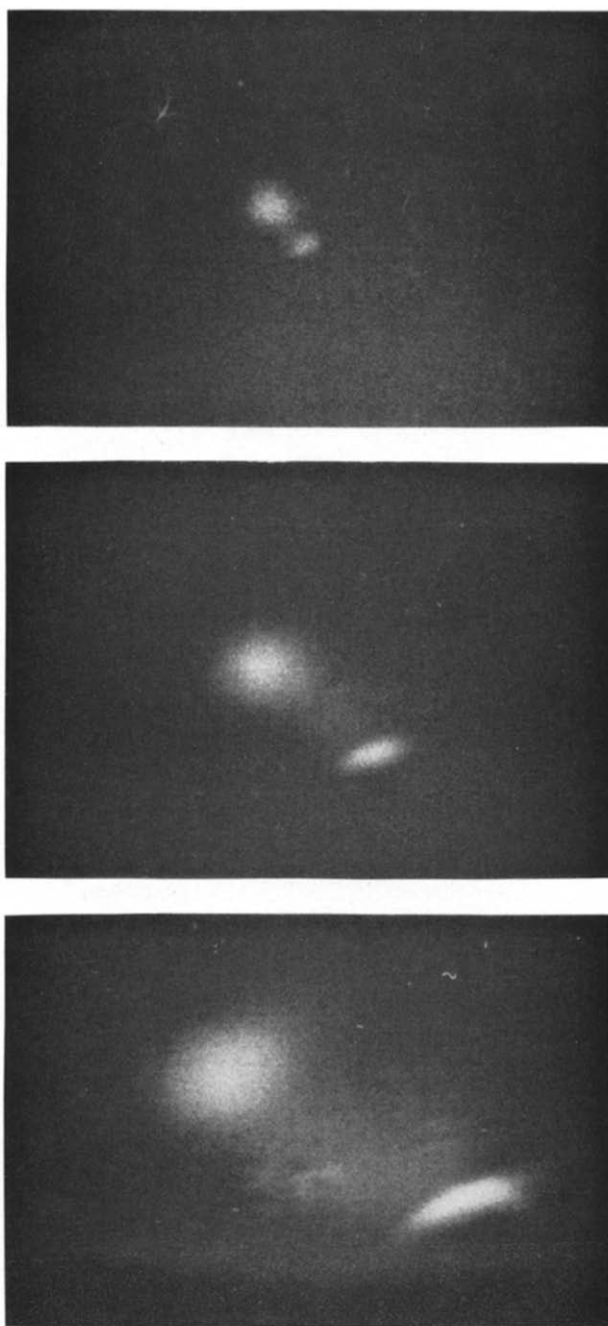


FIG. 3. (d). THE Sr I AND Ba II CLOUDS OF NOVEMBER 27, 1964, 2 min 44 sec, 7 min 3 sec AND 12 min 25 sec AFTER EVAPORATION.

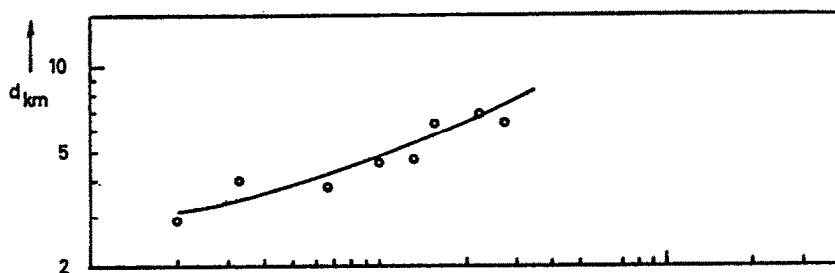


FIG. 3. (a). DIAMETER $d^{0.5}$ OF THE CLOUD OF NOVEMBER 27, 1964, IN Sr I AS A FUNCTION OF TIME.

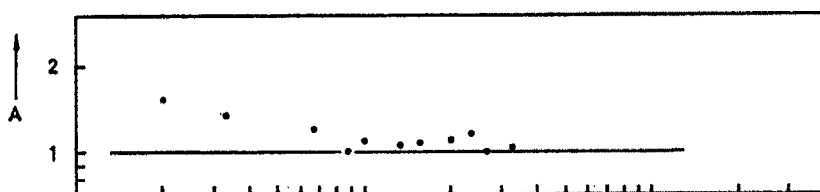


FIG. 3. (b). ASYMMETRY FACTOR A AS A FUNCTION OF TIME.

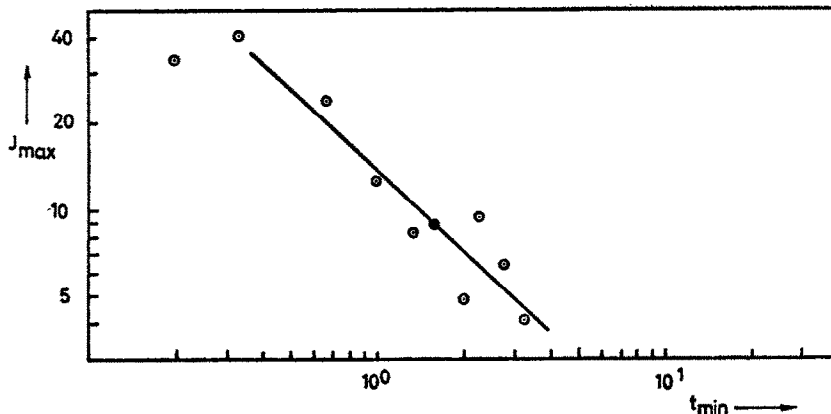


FIG. 3. (c). MAXIMUM INTENSITY OF THE CLOUD IN Sr I LIGHT OF AS A FUNCTION OF TIME.
 ——— GEOMETRICAL DILUTION, $J_{\max} t^{-0.95}$ AND LEAST SQUARE FIT TO THE DATA.

6 min after evaporation; values for diffusion, initial radius and scale height, which are deduced from the growth of the diameter, are therefore uncertain. The flattening of the curve at the end of the observation can be explained by a downward drift of the cloud as a whole. Because of the small basis of triangulation for this experiment, this downward drift could not be verified.

The Sr-cloud 4 showed a displacement in the evolution of the diameter $d^{0.5}$ and especially $d^{0.75}$ (Fig. 2a). This can be explained by the transition from the optically thick to the optically thin case. This assumption is also supported by the behaviour of the asymmetry

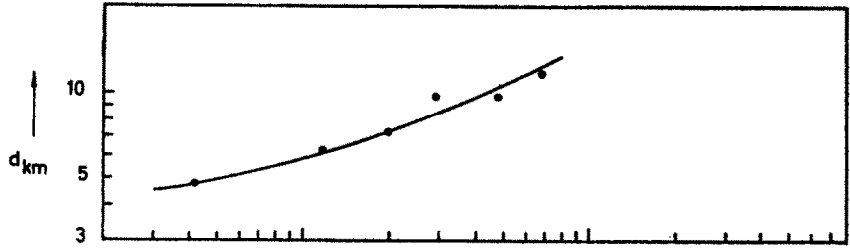


FIG. 4. (a). DIAMETER $d^{0.5}$ OF THE CLOUD OF NOVEMBER 27, 1964, IN Ba I LIGHT AS A FUNCTION OF TIME.

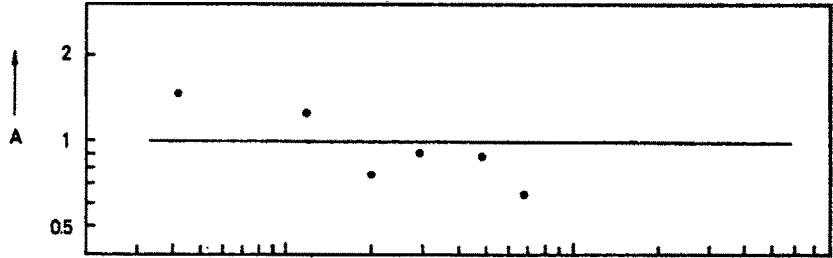


FIG. 4. (b). ASYMMETRY FACTOR A AS A FUNCTION OF TIME.

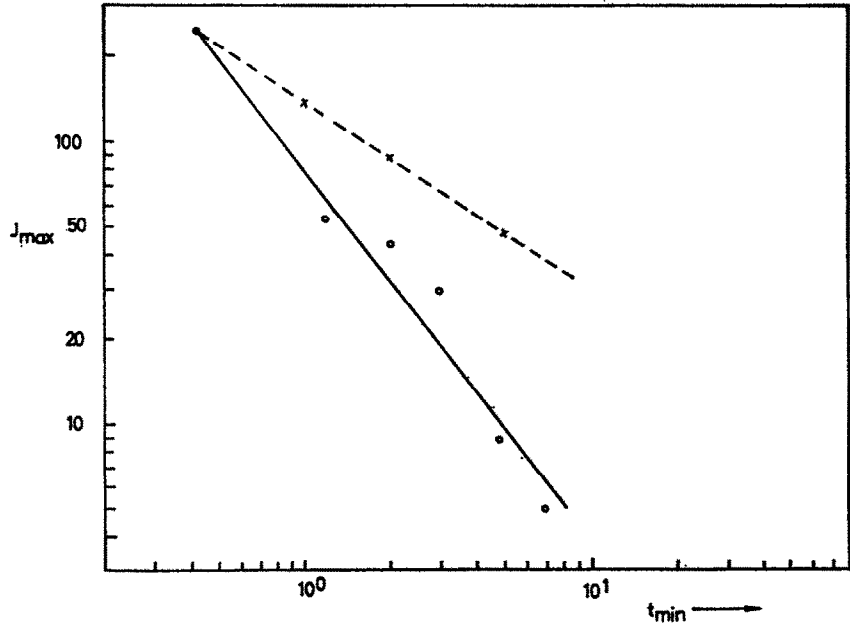


FIG. 4. (c). MAXIMUM INTENSITY OF THE CLOUD IN Ba I LIGHT AS A FUNCTION OF TIME.
— — — GEOMETRICAL DILUTION, $J_{\text{max}} t^{-0.66}$
— — — LEAST SQUARE FIT TO THE DATA.

factor (Section 8c) which becomes unity at about the same time. Afterward the cloud has a symmetrical shape.

In Fig. 5 the diffusion coefficient is listed versus height. Included in this Figure are values from experiments carried out at heights of 125 km and 200 km. Figure 5 shows the enhanced diffusion of ionized barium along the lines of the Earth's magnetic field.

(b) *The central intensity*

In Figs. 1c, 2c, 3c and 4c the maximum intensity of the clouds are given as a function of time. The intensity of the Sr cloud 3 obtained its full value about 6 min after evaporation

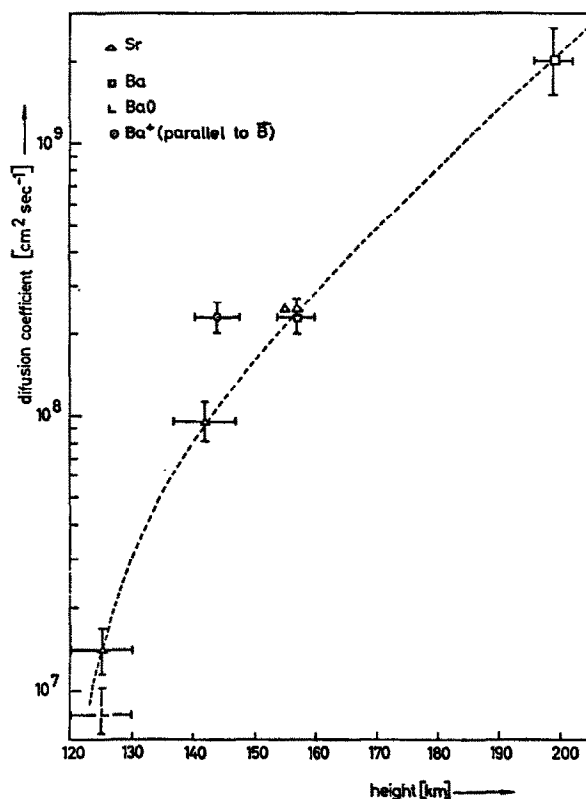


FIG. 5. DIFFUSION COEFFICIENT OF Ba, Sr AND Ba⁺ VS. HEIGHT.

and remained constant through the whole period of observation. This shows that the cloud remained optically thick.

Due to sunrise the intensity of this cloud increased by a factor of 10 during about 3 min. This rate was much greater than the rate of decrease in intensity at sunset. The reason for this is not yet understood. Absorption of the Sr by the atmosphere can be excluded as indicated by the shape of the intensity curve. Perhaps the solar radiation in the relevant range of wavelengths is attenuated at a smaller solar depression angle in the evening than in the morning.

(c) *The shape of the clouds*

In Figs. 1b, 2b, 3b and 4b the asymmetry factor A is plotted versus time. This factor is defined as

$$A = \frac{(r^{0.5} - r^{0.75})_{\text{away from Sun}}}{(r^{0.5} - r^{0.75})_{\text{toward Sun}}}$$

The radii $r^{0.5}$ and $r^{0.75}$ are drawn from the point of the maximum intensity of the cloud away from the Sun and toward the Sun, respectively, provided that the line of sight is nearly perpendicular to the Sun-cloud line. As long as the cloud is optically thick, the asymmetry factor A should be greater than unity. When the cloud becomes optically thin, the factor A should approach unity. According to Fig. 1b the cloud was asymmetrical during the whole observation period. It remained optically thick. After Fig. 2b the transition took place about 8 min after evaporation, in accordance with the displacement in the curve of $d^{0.75}$. The cloud was flattened in the vertical direction as shown in Fig. 2d. This effect is perhaps a consequence of the downward motion and the vertical gradient of the diffusion coefficient.

The asymmetry factor A seems to be a good measure of the transition in optical thickness because it is independent of the intensity of the solar radiation.

The evolution of the ion clouds is determined by the Earth's magnetic field. The diffusion perpendicular to the field is inhibited. Therefore the ion clouds which are produced immediately after the evaporation become cigar-shaped and map out the direction of the Earth's magnetic field. The ion cloud of Fig. 3 is distorted at its lower end (corresponding to the upper end of the Figure), which has a height of 135 km. This distortion is mainly attributed to a shear of the horizontal winds and the variation of the collision frequency over the extension of the cloud.

9. MOTION OF THE CLOUDS

(a) *Neutral clouds*

Measurements of the motion of neutral metal vapour clouds allows one to determine wind velocities of the neutral component of the atmosphere. The results are summarized in Table 6.

TABLE 6

No.	Height (km)	Horiz. vel. (msec ⁻¹)	Vertic. vel. (msec ⁻¹)	Direction	Element	Date	Time	Place
—	125	55–90	—	South-east	Sr/BaO	21.5.63	19.30 UT	Sahara
3	142	60	—	South	Sr	15.2.64	5.50 UT	Sahara
4	157–140	75	–13	South	Sr	6.7.64	20.23 CET	Sardinia
6	152–161	75	+15	North-east	Ba/Sr	27.11.64	17.38 UT	Sahara
7	164–152	74	–30	North-east	Ba/Sr	30.11.64	17.37 UT	Sahara
8	200–177	130	–30	North-east	Ba	30.11.64	17.37 UT	Sahara

(b) *Ionized clouds*

The velocities of the ion clouds are listed in Table 7 together with the velocities of the neutral clouds. Figures 6 and 7 show the movement of ionized and neutral clouds projected in a horizontal plane. The interpretation of these results and particularly the derivation of electric fields from these motions are discussed in another paper (Haerendel *et al.*, 1966).

TABLE 7

No.	Height (km)	Horiz. vel. (msec ⁻¹)	Vertic. vel. (msec ⁻¹)	Vel. _⊥ * (msec ⁻¹)	Vel. * (msec ⁻¹)	Element	Data	Time (UT)	Place
6	152-161	75	+15	74	7,8	Ba/Sr	27.11.64	17.38 UT	Sahara
6	152-144	39	-15	26	32	Ba ⁺	27.11.64	17.38 UT	Sahara
7	164-152	74	-30	73	34	Ba/Sr	30.11.64	17.37 UT	Sahara
7	159-148	51	-15	47	23	Ba ⁺	30.11.64	17.37 UT	Sahara
8	199-178	130	-30	118	58	Ba	30.11.64	17.37 UT	Sahara
8	199-166	66	-47	52	63	Ba ⁺	30.11.64	17.37 UT	Sahara

* Vel._⊥ and Vel._{||} are the velocities perpendicular and parallel to the major axis of the ionized Ba-clouds.

10. THE HIGH-ALTITUDE EXPERIMENT OF DECEMBER 3, 1964

The experiment of December 3, 1964, took place at a height of 385 km. A mixture of $\text{Sr}(\text{NO}_3)_2 + 6 \text{ Mg}$ which was successfully tested on February 14 and 15, 1964, was used. The cloud evolved spherically and eventually became greater than the aperture angle of the cameras (50°). The true diameter of the cloud was finally probably more than 400 km.

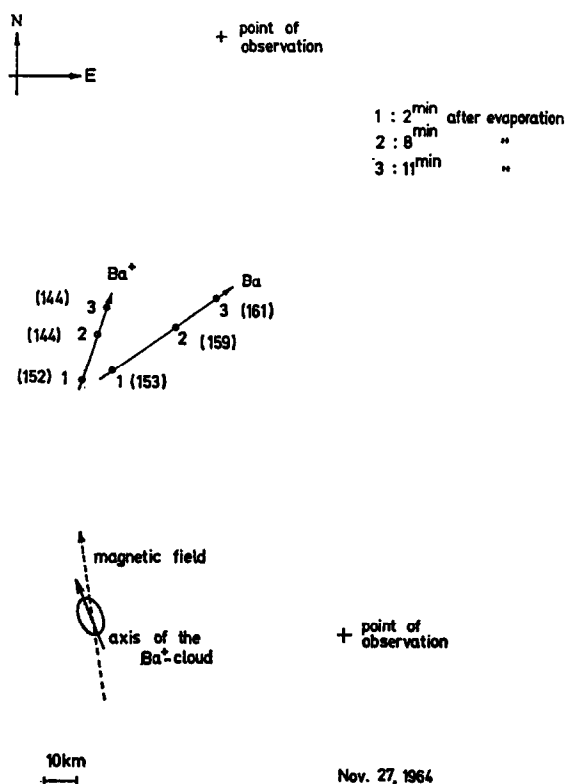


FIG. 6. GROUND-PLANE OF THE MOVEMENT OF THE CLOUDS OF NOVEMBER 27, 1964, CREATED AT 152 km.

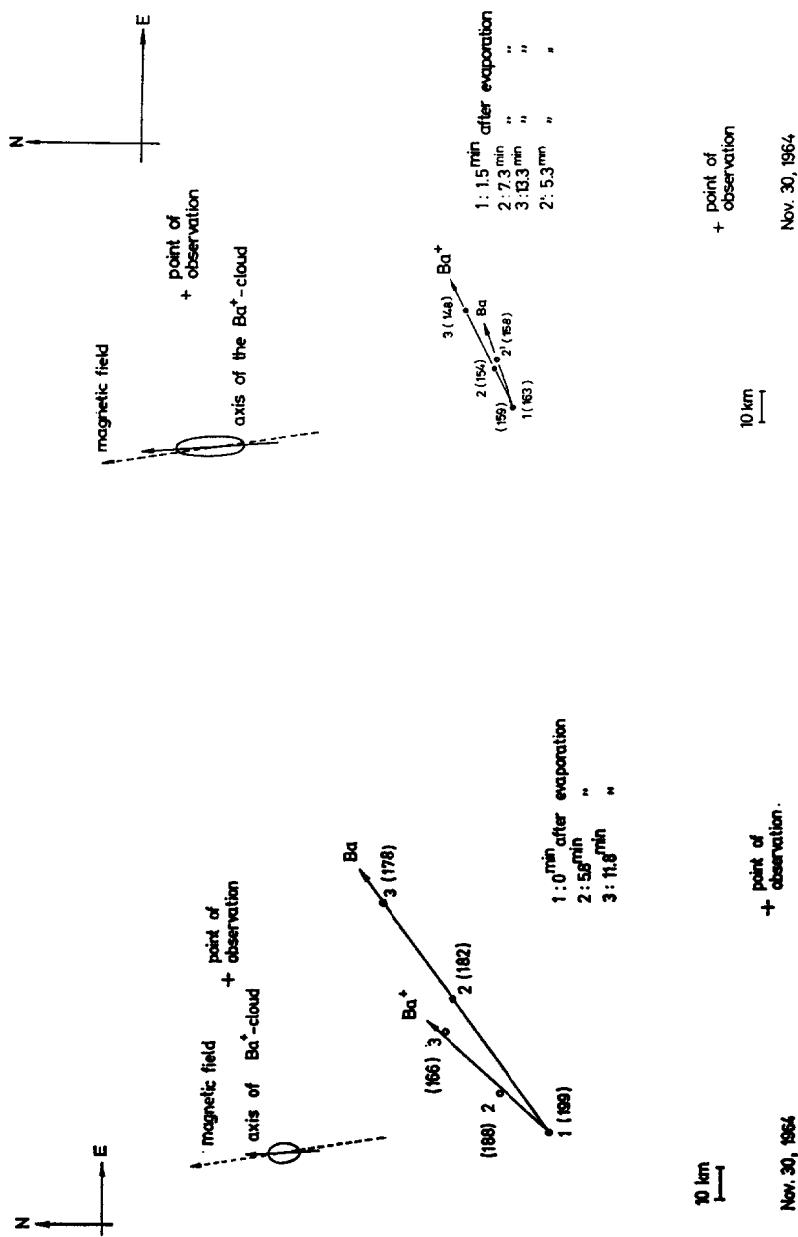


FIG. 7. (b). GROUND-PLANE OF THE MOVEMENT OF THE CLOUDS OF NOVEMBER 30, 1964, CREATED AT 200 km.

FIG. 7. (a). GROUND PLANE OF THE MOVEMENT OF THE CLOUDS OF NOVEMBER 30, 1964, CREATED AT 164 km.

The evolution of the cloud was studied in the initial phase. As seen in Fig. 8 a high expansion velocity of about 3.8 km sec^{-1} was obtained which is over 4 times greater than the mean thermal velocity of the atoms at a temperature of 3000°K . About 8 sec after the explosion the expansion velocity decreased due to the collisions of the Sr atoms with atmospheric particles. From this a mean free path of about 30 km can be deduced. About 23 sec after evaporation the cloud was in equilibrium with the atmosphere.

The expansion of the cloud was investigated theoretically. Model calculations taking into account the non-stationary expansion of an ideal gas of Sr starting with an initial

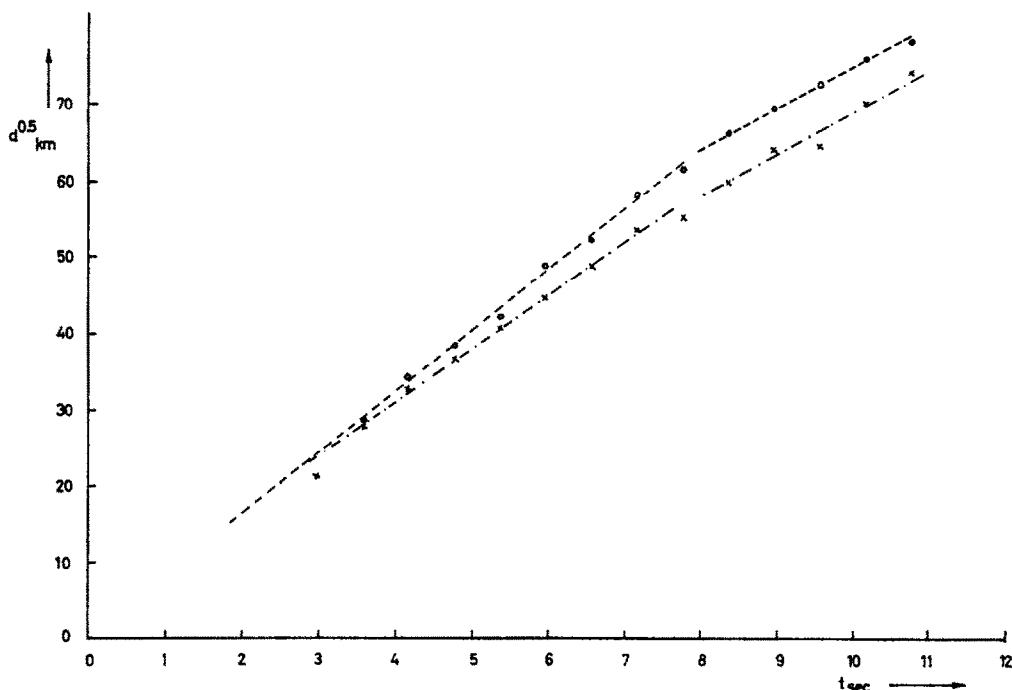


FIG. 8. EXPANSION OF THE Sr CLOUD OF DECEMBER 3, 1964 IN THE INITIAL PHASE IN EAST-WEST (○ ○ ○ ○) AND NORTH-SOUTH (× × × ×) DIRECTION. HEIGHT OF THE EVAPORATION 385 km.

temperature of 3000°K give typical expansion rates of 1 km sec^{-1} . With an additional heating due to collisions with hot dust particles which emerge from the reaction and may consist of MgO , one obtains an expansion velocity of 2 km sec^{-1} and an indication of a central hole which is apparent on the photographs. These investigations will be published in a separate paper (Giese and Smilga, 1966).

11. CONCLUDING REMARKS

The experiment carried out on November 27, 1964 was the first to give measurable amounts of evaporated neutral and ionized Ba. Since then other experiments have been carried out, so that we now have four different chemical mixtures for the evaporation of Ba atoms in measurable quantities. The best yield was obtained with a mixture of $\text{CuO} + \text{Ba}$. But in contrast to the evaporation of Sr, where yields of 30 per cent and more were reached, only a few per cent of evaporated Ba was obtained. Further studies to be carried out with the $\text{CuO} + \text{Ba}$ -mixture are mainly aimed at an enhancement of the Ba yield.

REFERENCES

- FÖPPL H., HAERENDEL G., LOIDL J., LÜST R., MELZNER F., MEYER B., NEUSS H. and RIEGER E. 1965. *Planet. Space Sci.* **13**, 95.
GIESE R. H. and SMILGA W. 1966. To be published.
HAERENDEL G., LÜST R. and RIEGER E. 1967. *Planet. Space Sci.* **15**, 155.
HAERENDEL G. and SCHOLER M. 1966. Presented at COSPAR, Vienna.
HASER L. 1966. To be published.
HUDSON R. D. 1965. Private communication.
LÜTJENS P. 1966. Diplomarbeit, Univ. Munich.

Резюме—Обсуждаются опыты с испускаемыми парами стронция и бария в верхние слои атмосферы, проведенные в Сахаре и Сардинии в 1964г.

(1) Выход выпаренного металла испытывался на предмет различных химических реакций. У стронция обнаружилось отдачи до 40%. Что касается бария, самые лучшие результаты были получены смесью CuO с Ba , с выходом в почти 1%.

(2) Испытания не обнаружили никаких ионов стронция, тогда как барий сильно ионизирован. Ионизация распространяется двумя различными стадиями: во время начальной фазы, с характерной скоростью в примерно 5 сек. и путем более медленного процесса фотоионизации, с характерной скоростью в пригл. 100 сек.

(3) Диаметр нейтральных облаков увеличился, как и предвиделось, исключительно для молекулярной диффузии.

(4) Скорость увеличения в центральной интенсивности облаков на восходе Солнца превышала скорость уменьшения на заходе Солнца.

(5) Скорости атмосферного ветра, в $50\text{--}430\text{ мсек}^{-1}$, определялись из движения нейтральных облаков. Движение ионных облаков, перпендикулярное магнитному полю Земли, указывало на присутствие электрических полей.

(6) Исходное распространение скорости для взрывчатых смесей превышало среднюю тепловую скорость атомов коэффициентом в 4, при температуре в приблизительно 3000°K .